Template Synthesis and Electrochemical Characterization of Nickel-Based Tubule Electrode Arrays

Yu-Li Tai and Hsisheng Teng*

Department of Chemical Engineering, National Cheng Kung University, Tainan 70101, Taiwan

Received June 10, 2003. Revised Manuscript Received November 7, 2003

A nickel-based tubule electrode array was fabricated by using electroless deposition with a polycarbonate membrane serving as a template. Hypophosphite was the reducing agent in the Ni deposition, and electrodes made of a Ni−P alloy were formed. The tubule has an internal diameter of ca. 180 nm, a wall thickness of ca. 20 nm, and a length of ca. 2 μm. The electrode array provided an exposed area ca. 8.8 times as large as that of a planar electrode, suggesting a potential application of the array in sensor devices. Cyclic voltammetric measurements in KOH showed that the electrochemical response from the $Ni(OH)_2$/NiOOH redox reaction for the electrode arrays was more than 40 times larger than that for an planar electrode. The nanoscale structure of the tubule was concluded to be responsible for this magnification of the redox response. Heat treatment combined with overcharge oxidation of the electrode arrays was found to significantly improve the charge storage capacity resulting from the redox reaction. The present work has provided important concepts capable of improving the performance of a nickel hydroxide electrode for nickel metal hydride batteries.

Introduction

Nanomaterials have properties (e.g., optical, electronic, magnetic, etc.) differing from those of a macroscopic sample of the same material.[1] Porous media containing nanoscale pores have been used as substrates for preparing nanomaterials.[2−7] Using nanoporous membranes as templates for preparing nanoscopic metal fibrils was demonstrated decades ago.[8] The application of this method for the fabrication of a variety of micro- and nanomaterials has been conducted by numerous research groups recently.[2,3,9−12] Because the membranes employed have cylindrical pores of uniform diameter, a nanosize cylinder or fibril of the desired material is obtained in each pore. The thus-derived cylinder or fibril can be solid or hollow, depending on the technique employed in synthesis.

This template synthesis method has been applied to materials such as conductive polymers,[2,3] semiconductors,[12] metals,[13−15] and carbon.[16] Depending on the usage, the prepared nanostructures can be constructed with a variety of architectures.[4] In the present work, an electrode with an exposed area much larger than that of a planar electrode is intended to be prepared. The magnitude of the current signal or charge stored resulting from the electrode reactions can thus be magnified due to the extended electrode area. Such an electrode can be used as substrate for solution/gas sensors or battery electrodes. In accord with this demand, an ensemble of metallic micro- or nanostructures that protrude from the electrode surface like the bristles of a brush are synthesized with the template method.

Metal can be deposited within the pores of the template membranes by either electrochemical or chemical (i.e., electroless) reduction of an appropriate metal ion.[9,16] Electrochemical deposition is accomplished by coating one face of the membrane with a metal film and using this metal film as a cathode for electroplating. Only solid cylinders can be prepared from this deposition.[17] As for electroless deposition of metal within the pores of the template membrane, a catalyst must be applied to the pore wall,[18] and hollow tubules are obtained with brief deposition times. Longer deposition times would cause filling-up of these tubules to form

* To whom correspondence should be addressed. Phone: 886-6-2385371. Fax: 886-6-2344496. E-mail: hteng@mail.ncku.edu.tw.

(1) Martin, C. R. *Acc. Chem. Res.* **1995**, *28*, 61.
(2) Martin, C. R. *Adv. Mater.* **1991**, *3*, 457.
(3) Martin, C. R.; Parthasarathy, R. V. *Adv. Mater.* **1995**, *7*, 487.
(4) Martin, C. R. *Science* **1994**, *266*, 196.
(5) Qin, D. H.; Lu, M.; Li, H. L. *Chem. Phys. Lett.* **2001**, *350*, 51.
(6) Honda, K.; Rao, T. N.; Tryk, D. A.; Fujishima, A.; Watanabe, M.; Yasui, K.; Masuda, H. *J. Electrochem. Soc.* **2000**, *147*, 659.
(7) Zhang, Z.; Dai, S.; Blom, D. A.; Shen, J. *Chem. Mater.* **2002**, *14*, 965.
(8) Possin, G. E. *Rev. Sci. Instrum.* **1970**, *41*, 772.
(9) Brumlik, C. J.; Menon, V. P.; Martin, C. R. *J. Mater. Res.* **1994**, *9*, 1174.
(10) Huber, C. A.; Huber, T. E.; Sadoqi, M.; Lubin, J. A.; Manalis, S.; Prater, C. B. *Science* **1994**, *263*, 800.
(11) Tonucci, R. J.; Justus, B. L.; Campillo, A. J.; Ford, C. E. *Science* **1992**, *258*, 783.
(12) Hiruma, K.; Yazawa, M.; Katsuyama, T.; Ogawa, K.; Haraguchi, K.; Koguchi, M.; Kakibayashi, H. *J. Appl. Phys.* **1995**, *77*, 447.
(13) Chakarvarti, S. K.; Vetter, J. *Nucl. Instrum. Methods Phys. Res.* **1991**, *B62*, 109.
(14) Nishizawa, M.; Menon, V. P.; Martin, C. R. *Science* **1995**, *268*, 700.
(15) Vetter, J.; Spohr, R. *Nucl. Instrum. Methods Phys. Res.* **1993**, *B79*, 691.
(16) Parthasarathy, R. V.; Phani, K. L. N.; Martin, C. R. *Adv. Mater.* **1995**, *7*, 896.
(17) Brumlik, C. J.; Martin, C. R. *Anal. Chem.* **1992**, *64*, 1201.
(18) Menon, V. P.; Martin, C. R. *Anal. Chem.* **1995**, *67*, 1920.

10.1021/cm030430z CCC: $27.50
Published on Web 12/19/2003

solid fibrils. Hollow tubule structures that have larger exposed areas are expected in the present work.

It has been well-known that the electroless Ni−P coating has a highly even plating capability, as well as high bonding strength and electrical conductivity.[19] These properties present the potential applications of this coating in sensor devices and nickel metal hydride batteries. Thus, electrodes with hollow Ni−P bristles protruding from a planar surface are fabricated using commercially available polymer membranes as the template. The resulting electrodes are subjected to electrochemical analysis, in an attempt to appraise the applicability of the electrodes in magnifying the signal of surface reactions as well as the capacity of charge storage.

Experimental Section

Electrode Preparation. Polycarbonate membranes from Millipore are used as the template in Ni-based electrode synthesis. These membranes have a pore diameter of ca. 200 nm and a mean thickness of ca. 10 μm. Electroless deposition is employed in an attempt to coat a Ni thin film over the pore walls and the faces of the membrane. Electroless metal deposition involves the use of a chemical reducing agent to plate a metal from solution onto a surface. Before plating, the membrane was cleaned by methanol to remove any oil and salts. A sensitizer (Sn^{2+}) was applied to the membrane surface by immersing the membrane in a 50:50 methanol/water solution containing 0.026 M $SnCl_2$ and 0.07 M trifluoroacetic acid for 30 min. After sensitization the membrane was rinsed thoroughly with deionized water and then activated by immersion in an aqueous solution of 0.25 g/L $PdCl_2$ and 1.0 g/L HCl. This caused a redox reaction in which the surface-bound Sn^{2+} was oxidized to Sn^{4+} and Pd^{2+} was reduced to elemental Pd with deposition on the surface. The membrane was then rinsed with water.

After Pd deposition, the membrane was immersed in a Ni-plating solution at 88 °C for 30 min. The solution contained $H_2PO_2^{-1}$ as the reducing agent. After plating, the membrane was thoroughly rinsed with water and air-dried. Dichloromethane was used to dissolve the polycarbonate membrane, and a Ni−P electrode array (NPEA) was thus obtained. The reverse side of the NPEA can serve as a planar electrode (PE). The as-deposited electrodes were heat treated at 250−400 °C under helium flow. This treatment is expected to vary the crystalline structure of the Ni−P electrode and thus the electrochemical behavior.

Electrode Characterization. A scanning electron microscope (SEM) was used to study the surface features of the NPEA. The chemical composition of the electrodes was analyzed by using the energy-dispersive X-ray spectrum (EDS). X-ray diffraction (XRD) patterns were obtained by using a Rigaku X-ray diffractometer that employed a copper target.

Electrochemical measurements were carried out in 0.5 M KOH to analyze the electrochemical behavior of the Ni-based electrodes. In the measurements a Pt wire was used as the counter electrode and a saturated calomel electrode (SCE) was used as the reference. Epoxy was employed to seal the electrode with a geometric area of ca. 0.36 cm^2 to contact with the electrolyte solution. Potential-sweep cyclic voltammetric measurements were conducted between −0.7 and 0.7 V at a scan rate of 10 mV/s. Galvanostatic charge/discharge within 0−0.6 V was performed at 2 mA to estimate the charge storage capacity of the electrodes.

Results and Discussion

Physical Characteristics of the Ni−Based Electrodes. Figure 1a shows a SEM image of the NPEA that

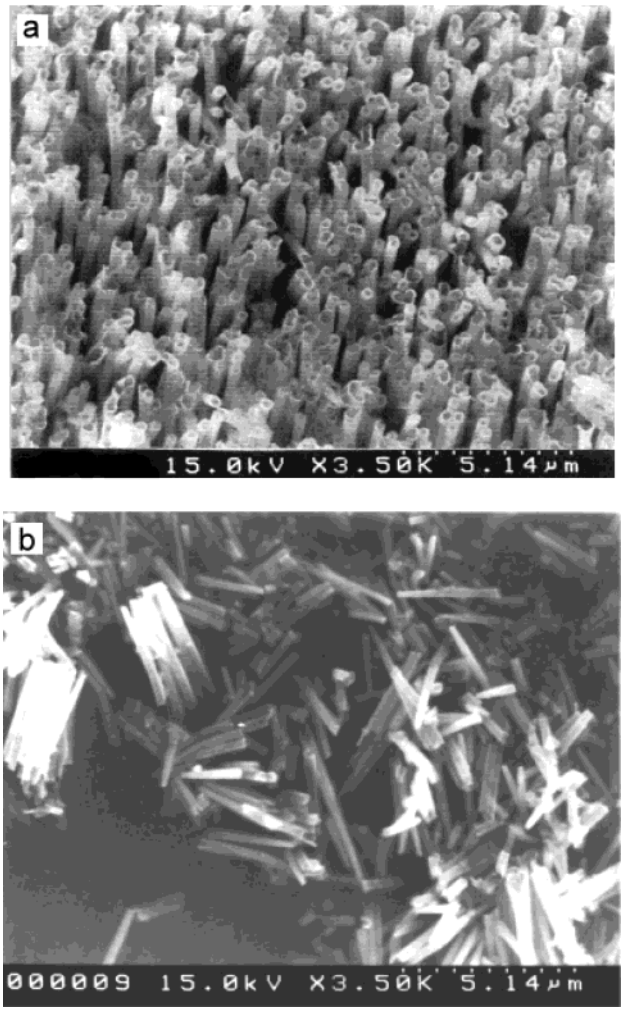

Figure 1. SEM micrographs of (a) the Ni−P electrode array (NPEA) and (b) the scraped-off tubes.

was fabricated using the template synthesis described above. It can be seen that the standing bristle-like electrodes are hollow. The bristles can be scraped off, and tubes of ca. 2 μm long can be obtained (Figure 2b). On the basis of the SEM image, the tubes have an internal diameter of ca. 180 nm and a wall thickness of ca. 20 nm. The schematic diagram in Figure 2 summarizes the progression of the NPEA synthesis stagewise. Stage 1 shows that the polycarbonate membrane has cylindrical pores distributed across the membrane surface. The pore density of the membrane is ca. 3×10^8 pores/cm^2, which is evaluated from the SEM image. The surface of the membrane was then deposited with Sn^{2+} after sensitization and with Pd after activation (see stage 2). In the process of electroless deposition with Ni, because of the high deposition rate, the pore entrance was sealed before the Ni layer could fully cover the surface of the pore walls. Thus, a limited length of Ni tubules can be formed along the pore axes (see stage 3). The length of the Ni tubules can be controlled by regulating the rate of deposition, through the adjustment of the temperature and reagent concentrations. After dissolution of polycarbonate in the Ni-deposited membrane with dichloromethane, a piece of bristle-like NPEA (see stage 4) can be obtained from each side of the template membrane employed. Assuming that the bristle-like electrodes are hollow cylinders with uniform

(19) Mencer, D. *J. Alloys Compd.* **2000**, *306*, 158.

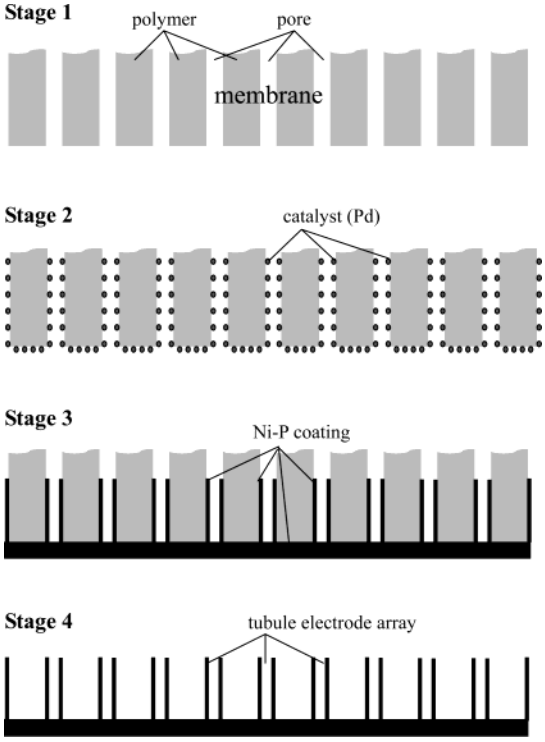

Figure 2. Scheme for the synthesis of Ni−P electrode array (NPEA) using polymer membrane as template.

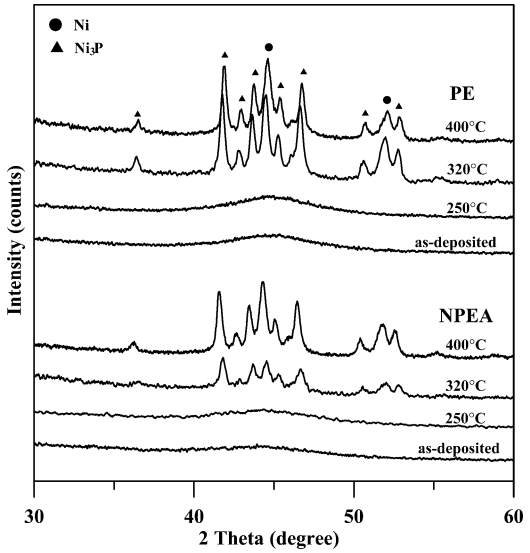

Figure 3. X-ray diffraction patterns of the Ni−P electrode arrays (NPEAs) and planar electrodes (PEs) heat-treated at different temperatures.

inside diameter, the exposed surface area of NPEA was estimated by calculation to be ca. 8.8 times as large as that of a planar surface.

Figure 3 shows the X-ray diffraction patterns of the NPEA and PE treated at different temperatures. Only a weak and broad Ni (111) peak can be seen for the as-deposited NPEA and PE and those treated at 250 °C. This is in agreement with previous research,[20] demonstrating that microcrystalline and amorphous phases coexist in the Ni−P alloys that have been treated at temperatures lower than 300 °C. The solid solubility of phosphorus in nickel is, as a matter of fact, negligibly

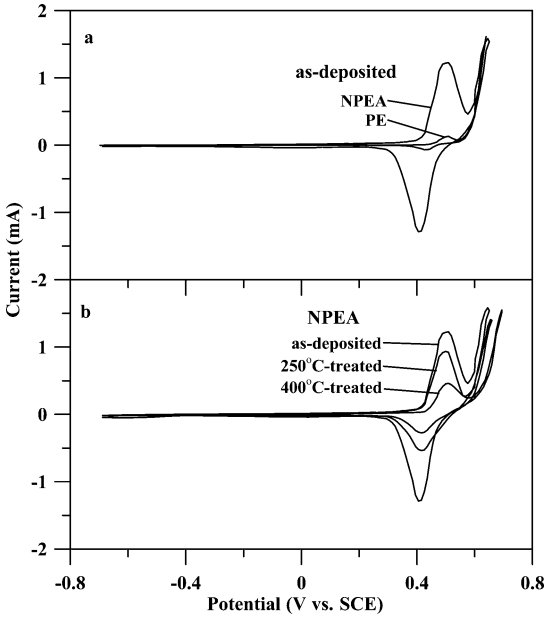

Figure 4. Comparison of the second-cycle voltammograms for different electrodes (0.36 cm^2): (a) the as-deposited NPEA and PE; (b) the NPEAs treated at different temperatures.

low based on the Ni−P binary phase diagram. The smaller atomic radius of P compared to that of Ni may be responsible for the accommodation of P in the Ni lattice,[21] allowing the formation of the metastable Ni−P film. It has been reported in another study[22] that the crystalline structure of the deposited Ni−P alloy is related to the P content. The chemical composition of the NPEA was analyzed using EDS, showing a P content of ca. 7−9 wt %. With this content, the as-deposited Ni−P is suggested to consist of a fine dispersion of microcrystalline Ni in an amorphous matrix,[22] in agreement with the results reflected in the XRD patterns shown in Figure 3.

Although the XRD data show that the crystalline structure of the deposited Ni−P alloy was insensitive to the heat treatment at low temperatures (<250 °C), a significant increase in Ni grain size and the formation of an intermetallic compound, Ni_3P, were observed when these electrodes were heat-treated at higher temperatures (>320 °C), as depicted in Figure 3. It is of interest to observe from the XRD patterns that more ordered Ni and Ni_3P phases are formed in PE than in NPEA for heat treatment at 320 °C. This result can be attributed to the nanoscale wall thickness of the NPEA (20 nm), which would impose difficulties on the formation of large crystallites due to the high surface-area-to-volume ratio of nanomaterials.

Electrochemical Behavior of the Ni−Based Electrodes. Potential sweep cyclic voltammetry was employed to analyze the electrochemical response of the NPEAs and PEs. Figure 4a shows the second-cycle voltammograms of the as-deposited PE and NPEA measured at a sweep rate of 10 mV/s. In the low-potential regime ranging between −0.7 and 0.1 V both of the electrodes are stable, and the capacitive currents, mainly resulting from the double-layer mechanism, are

(20) Tzeng, S. S.; Chang, F. Y. *Thin Solid Films* **2001**, *388*, 143.

(21) Lambert, M. R.; Duquette, D. J. *Thin Solid Films* **1989**, *177*, 207.

(22) Ma, E.; Luo, S.; Li, P. *Thin Solid Films* **1988**, *166*, 273.

negligibly small compared to the peak currents at high potentials. The capacitive currents can be employed to estimate the ratio of the real exposed areas of NPEA and PE. The ratio of the capacitive currents for these two electrodes was found to be similar to that of their calculated exposed areas (i.e., 8.8 for NPEA to PE). This agreement indicates the similarity of the textural features of these two electrodes.

In the high potential regime, there are obvious peak currents due to redox reaction pairs occurring near 0.50 and 0.41 V for the anodic and cathodic sweeps, respectively. The peak currents of PE are much smaller than those of the NPEA. These peaks in the voltammogram correspond to oxidation and reduction of the active material according to the reaction[23]

$$Ni(OH)_2 + OH^- \leftrightarrow NiOOH + H_2O + e^- \quad (R1)$$

For potentials larger than 0.6 V, a steep rise of current with the potential can be seen for both the electrodes which corresponds to the occurrence of oxygen evolution reaction according to[24]

$$4\ OH^- \rightarrow O_2 + 2\ H_2O + 4\ e^- \quad (R2)$$

In practical application of these electrodes to nickel metal hydride batteries, the electrochemical operation in alkaline solutions should be optimized in order to include the majority of the $Ni(OH)_2$/NiOOH reversible redox reaction while minimizing the effect of oxygen evolution. Because of the high charge capacity, the electrode array shows a clear superiority over the planar electrode in this application.

Figure 4b shows the cyclic voltammograms of the NPEAs treated at different temperatures. It can be seen that the redox peak currents are suppressed upon heat treatment. The larger peak currents for the lower-temperature-treated NPEAs indicates a higher population of $Ni(OH)_2$ formed on the electrode surface. The larger proportion of Ni amorphous phase in the low-temperature NPEAs may cause the higher degree of Ni oxidation to form $Ni(OH)_2$ in alkaline solution.[25] It is generally recognized that metals in an amorphous phase are more reactive than those in their crystalline structure, because atoms in three-dimensional space without long-range order are allowed for interaction possibilities (with other species) not found in crystals.[26]

It has been reported that overcharging of a nickel hydroxide electrode, thus leading to oxygen evolution, would affect the electrochemical behavior of the electrode that undergoes reactions according to R1.[24] Multi-cyclic voltammetry was conducted with the NPEAs, and the results for the as-deposited and 400 °C-treated NPEAs are illustrated in Figure 5 as typical examples. One can observe from Figure 5a that the peak currents of the as-deposited NPEA increase upon increasing the cycle number of the potential sweep. It is obvious that

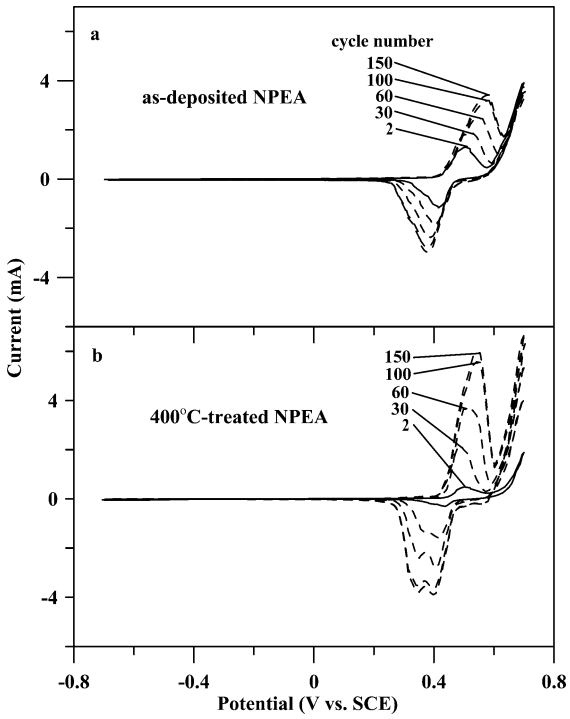

Figure 5. Cyclic voltammograms of the as-deposited (a) and 400 °C heat-treated (b) NPEAs (0.36 cm^2) obtained at different cycle numbers.

the oxidation of Ni to form $Ni(OH)_2$ can be enhanced with this cyclic potential sweep process. The currents nearly stabilized after 100 cycles of the sweep, indicating that the $Ni(OH)_2$ film was thick enough at this point to retard further oxidation of Ni. No decrease in the current intensity was observed with this repeated cycling, although degradation of $Ni(OH)_2$ with repeated overcharging to cause reduction of the peak current was generally observed for ordinary planar electrodes.[24] The potential difference between the anodic and cathodic peaks was seen to increase with the cycle number, indicating that the resistance related to electrolyte migration, as well as to electrical conduction, was magnified with cycling due to the increasing thickness of $Ni(OH)_2$ film on the electrode surface.

Figure 5b shows the multi-cyclic voltammograms for the NPEA treated at 400 °C. The peak currents were found to increase more rapidly with cycle number than those for the as-deposited NPEA. After 100 cycles of scan, the peak currents of the 400 °C NPEA are larger than those of the as-deposited one, although they are smaller at low cycle numbers. For scans with low cycle numbers, the crystallinity of surface Ni determines the extent of Ni oxidation and thus the current value in cyclic voltammograms. However, for the scans with large cycle numbers, the current values are determined by how easily the $Ni(OH)_2$ film can grow and advance into the Ni tube walls through oxidation during the cycling. Therefore, the smaller stabilized currents of the as-deposited NPEA can be ascribed to the phosphorus atoms that are dispersed in the electrode, thus hindering the advancing of the $Ni(OH)_2$ into the Ni walls. With heat treatment to 400 °C, the phosphorus atoms become localized in the Ni_3P crystalline domain, and the oxidation of Ni to form $Ni(OH)_2$ can proceed with less hindrance. Similar to the situation for the as-deposited NPEA, the potential difference between the anodic and

(23) Srinivasan, V.; Weidner, J. W. *J. Electrochem. Soc.* **1997**, *144*, L210.
(24) Kim, H. S.; Itoh, T.; Nishizawa, M.; Mohamedi, M.; Umeda, M.; Uchida, I. *Int. J. Hydrogen Energy* **2002**, *27*, 295.
(25) Wu, M. S.; Huang, C. M.; Wang, Y. Y.; Wan, C. C. *Electrochim. Acta* **1999**, *44*, 4007.
(26) Ovshinsky, S. R. In *Physical Properties of Amorphous Materials;* Adler, D., Schwartz, B. B., Steele, M. C., Eds.; Plenum Press: New York, 1985; p 105.

Table 1. Accumulated Charge Stored Per Geometric Area Due to $Ni(OH)_2$/NiOOH Redox Reaction during the Anodic and Cathodic Potential Sweeps of the Stabilized NPEA and PE.

	as-deposited			400 °C heat-treated		
	NPEA	PE	ratio	NPEA	PE	ratio
anodic peak charge (mC/cm^2)	70	1.7	42	186	4.7	40
cathodic peak charge (mC/cm^2)	81	1.9	42	180	4.2	43

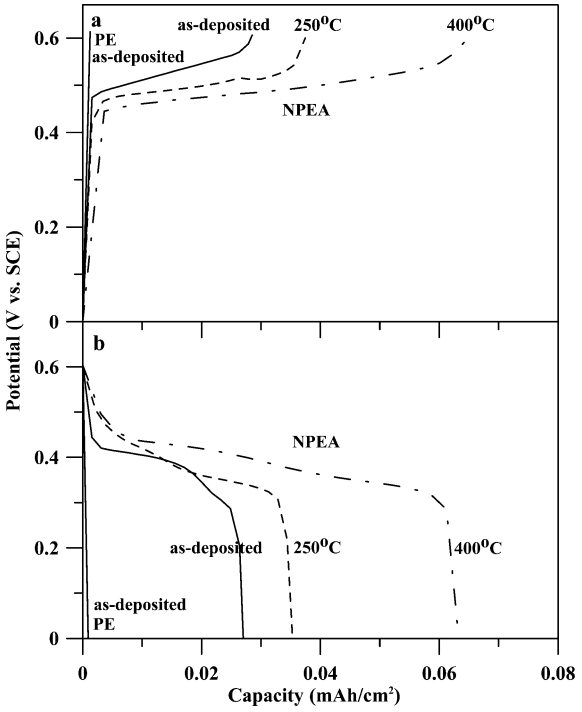

Figure 6. Comparison of galvanostatic charge (a) and discharge (b) curves for the different-temperature-treated NPEAs and the as-deposited PE obtained at 2 mA with electrode areas of 0.36 cm^2.

cathodic peaks of the 400 °C NPEA is an increasing function of the cycle number, reflecting the growth of $Ni(OH)_2$ film to cause insulation for electrical conduction and electrolyte migration. However, it is of interest that we observed the formation of two distinct cathodic peaks upon cycling. This may be attributable to the formation of nickel hydroxide of different phases (the β-phase would transfer to γ-phase upon overcharging[24]), thus leading to the difference in the reduction potential.

The charge stored per geometric area in the stabilized electrodes (after 100 times of cycling) corresponding to R1 can be calculated from integration of the cyclic voltammograms with the background subtracted, and the results are shown in Table 1. The capacity for NPEAs is much larger than that for PEs, ca. 42 times larger. The capacity ratio of NPEA to PE is larger than the exposed area ratio (ca. 8.8), indicating that the surface of NPEA is more reactive than that of PE in an alkaline solution environment. This high reactivity feature can be attributed to the fact that the NPEA structure contains a high proportion of surface atoms, which are more reactive than those in the bulk phase.

Figure 6 shows the galvanostatic charge/discharge curves of the stabilized PEs and NPEAs in KOH. The results in Figure 6 show that the NPEAs have capacities much higher than those of the planar electrodes, reflecting again the potential application of these electrode arrays to nickel metal hydride batteries. Heat treatment shows significant influence on the charge/discharge performance of the NPEAs. Both the charge and discharge capacities are seen to increase with the heat treatment temperature. Obviously, the extent of crystallization in the Ni−P layer affects the degree of Ni oxidation to $Ni(OH)_2$ and thus the charge storage capacity.

Summary and Conclusions

Nickel-based microelectrode arrays can be fabricated by electroless deposition using a polymer membrane as a template. Hollow tubule structures, instead of solid fibrils, are formed in the electrode array, and this feature makes this developed array a potential electrode for use in sensor or energy storage devices due to its high exposed surface area compared to that of a planar electrode.

Cyclic voltammetry in KOH showed that the electrochemical response per unit of exposed area for the $Ni(OH)_2$/NiOOH redox pair was much stronger from the electrode array than from the planar electrode, indicating that the nanoscale tubule structure has caused important influence on the reactivity of the electrode surface. On the other hand, the charge storage capacity due to double-layer mechanism was proportional to the exposed electrode area. Upon cyclic overcharge oxidation scanning the charge storage of the electrode array due to the redox pair was magnified without degradation, and this operation is beneficial for applying this electrode in nickel metal hydride batteries.

Heat treatment significantly affected the crystalline structure of the nickel-based electrodes. The electrode array was less sensitive to heat treatment than the planar electrode. The electrochemical response due to the redox pair was suppressed by heat treatment that results in crystallite formation. However, the overcharge oxidation scan was more efficient in magnifying the redox response of the heat-treated electrode array. For electrodes stabilized with the oxidation scan, the heat-treated electrode arrays have a higher redox charge capacity than the as-deposited array.

Athough the chemical composition of the nickel hydroxide electrodes for nickel metal hydride batteries is different from that of the electrode array prepared in the present work, the developed concepts in magnifying the $Ni(OH)_2$/NiOOH redox response, including electrode synthesis and some additional operations such as heat treatment and overcharge oxidation scan, have provided feasible methods to improve the energy storage in this application.

Acknowledgment. Financial support from the National Science Council of Taiwan is gratefully acknowledged (project NSC 91-2214-E-006-020).

CM030430Z